

Direct EELS observation of the oxidation states of Sm atoms in Sm@C_{2n} metallofullerenes (74 ≤ 2n ≤ 84)

Toshiya Okazaki

Department of Chemistry, Nagoya University, Nagoya 464-8602, Japan

Kazutomo Suenaga

Department of Physics, Japan Science and Technology Corporation, Meijo University, Nagoya 468-8502, Japan

Yongfu Lian and Zhennan Gu

Department of Chemistry, Peking University, Beijing 100871, People's Republic of China

Hisanori Shinohara^{a)}

Department of Chemistry, Nagoya University, Nagoya 464-8602, Japan

(Received 12 July 2000; accepted 8 September 2000)

The oxidation states of Sm atoms in various fullerene cages are directly investigated by electron energy-loss spectroscopy. The observed peak positions of the M_{45} edges of the Sm atom in Sm@C_{2n} [$2n = 74, 78, 80, 82$ (isomers I, III), 84 (isomers I, II, III)] are apparently shifted to the lower binding energy region in comparison with those of a trivalent Sm³⁺ in Sm₂O₃. The results indicate that the Sm atoms take +2 valence states irrespective of the fullerene cages. This observation is discussed based on a simple thermochemical cycle model. We also report that the Sm metallofullerenes have been converted to Sm carbide materials under a prolonged electron beam irradiation. © 2000 American Institute of Physics. [S0021-9606(00)01645-7]

I. INTRODUCTION

Endohedral metallofullerenes have attracted particular interests as they might exhibit unique solid-state properties associated with the charge transfer from metal atoms to carbon cages. The encapsulated metal effect on the charge distributions of metallofullerenes has been investigated by several experimental techniques.¹⁻⁶ In particular, the electronic structures of C₈₂-based monometallofullerenes have been studied extensively.¹ For example, the ultraviolet photoemission spectra of La@C₈₂ and Gd@C₈₂ showed characteristic features related to the trivalent $M^{3+}@C_{82}^{3-}$ (M =metal atom) state,^{2,3} whereas an x-ray photoemission study revealed the divalent character of the Tm atom in the C₈₂ fullerene cage.⁴ Based on these and the other systematic studies,⁷⁻¹⁰ it is now generally accepted that group 3 atoms (Y, La) and most of the lanthanide elements (Ce, Gd, etc.) donate three electrons to the C₈₂ cage (group A) while two valence electrons on group 2 (Ca, Sr, Ba) and the other lanthanide atoms (Sm, Eu, Tm, Yb) are transferred to the C₈₂ cage (group B).

The electronic states of di- and trimetallofullerenes were also studied by electron paramagnetic resonance (EPR)¹¹ and x-ray diffraction methods.^{12,13} In Sc₂@C₈₄, for example, Sc atoms are mutually separated from each other and locate close to the C₈₄ cage. The formal charge state of the Sc atom is +2, leading to the (Sc²⁺)₂@C₈₄⁴⁻ configuration.¹² Three Sc atoms in Sc₃@C₈₂ form an equilateral triangle cluster inside the carbon cage, and its electronic state is well represented by Sc₃³⁺@C₈₂³⁻.¹³

Under these circumstances, a control of the electronic structure of a metallofullerene by changing the size of the fullerene cage becomes progressively an important area of metallofullerene research. However, systematic studies of the electronic states of metallofullerenes with various sized fullerene cages have so far been limited. In a previous study, we have succeeded to isolate Sm-containing metallofullerenes with the fullerene cages from C₇₄ to C₈₄, and found that the oxidation state of the encapsulated Sm atom is +2 in Sm@C₈₂(II) as revealed by electron energy-loss spectroscopy (EELS).⁶

Here we report a systematic EELS measurement on a series of Sm metallofullerenes [Sm@C_{2n}, $2n = 74, 78, 80, 82$ (I, III), 84 (I, II, III)] to investigate the fullerene cage effect on their electronic structures. The peak positions of the Sm M_{45} edges of these molecules indicate that the Sm atoms take +2 states inside the fullerene cages; the intramolecular electron transfer process is not sensitive to the cage size nor the structure. This trend can be qualitatively explained by a simple thermochemical cycle. In addition, we also found that an extended or a strong irradiation of the electron beam leads to an increase of the trivalent features in the spectrum, indicating the destruction of the Sm metallofullerene, which will be eventually converted to the Sm carbide.

II. EXPERIMENT

Details of the synthesis and isolation of Sm-containing metallofullerenes were described previously.^{6,14} Briefly, the soot containing Sm metallofullerenes was produced by the DC arc-discharge method. Sm metallofullerenes were extracted by CS₂ and pyridine, and isolated by the multistep high-performance liquid chromatography (HPLC) method.⁸

^{a)}Author to whom correspondence should be addressed; electronic mail: nori@nano.chem.nagoya-u.ac.jp

The Sm metallofullerenes have structural isomers.⁶ The isomer [e.g., Sm@C₈₂(I)] was numbered in order of the increasing HPLC retention time.⁶ The purity of the Sm-containing metallofullerenes was >99%.

The EELS measurements were carried out under a transmission electron microscope (TEM) (JEOL 2010F) operated at 120 kV.^{6,15} The specimen was prepared by putting a few droplets of Sm metallofullerene/CS₂ solution on a holey carbon microgrid. The Sm metallofullerene was immediately dried up in the TEM chamber ($\sim 10^{-7}$ Torr). The EELS signals were recorded by an electron spectrometer with a charge coupled device (CCD) based detector (GIF, Gatan Imaging Filter). Great caution was taken to prevent electron irradiation effects during the valence state measurements. A small condenser aperture (20 μ m) was used to reduce the total current in the incident electron beam, and the region of interest (~ 30 nm) was chosen by the smallest selected area aperture, therefore the electron beam was not necessary tightly focused. In such a condition, the Sm M_{45} near-edge structure can be recorded in enough counting statistics with hardly any irradiation damage. Spectral evolution for the overdosed specimen (more than 60 s acquisition time under the present experimental conditions) will also be discussed in this article (see Sec. III).

The third electron affinities (E_a) of various fullerene cages were obtained by the semiempirical calculation (PM3) with the GAUSSIAN 98 program package.¹⁶

III. RESULTS AND DISCUSSION

A. EELS measurements on the Sm-containing metallofullerenes

High-energy spectroscopic methods such as x-ray absorption spectroscopy (XAS) and EELS can provide a direct proof of the valency of lanthanide ions.^{4,17,18} In particular, EELS is a powerful method to investigate the electronic properties of metallofullerenes because it can be performed in an electron microscope by using a tiny incident electron beam (typically a size of nanometer) and therefore requires only a small amount of specimen.¹⁵ Figure 1 shows the EELS spectra of a series of Sm metallofullerenes in the M_{45} edges region of Sm. A reference spectrum for a trivalent Sm³⁺ in Sm₂O₃ is also shown at the bottom of Fig. 1. The M_{45} spectra consist of two well-separated line groups due to the strong spin-orbit interaction (M_5 : $3d_{5/2} \rightarrow 4f_{7/2}$, M_4 : $3d_{3/2} \rightarrow 4f_{5/2}$).^{17,18} These lines are dominated by the $3d^{10}4f^n \rightarrow 3d^9 4f^{n+1}$ dipole transition and therefore reflect the $4f$ unoccupied density of states. The trivalent Sm³⁺ atom has an electronic configuration of $4f^5$ while that of the divalent Sm²⁺ is $4f^6$. This difference in the electronic state causes the 2~3 eV shifts in energy between the M_{45} peaks of Sm³⁺ and Sm²⁺.^{6,17,18}

The M_{45} edges of all the Sm-containing metallofullerenes currently studied appeared at the same energy positions within experimental accuracy (~ 1 eV) (Fig. 1). The highest positions for the M_{45} edges were observed at ~ 1105 and ~ 1078 eV. Apparently, these positions are shifted to the lower energy region in comparison with those of trivalent Sm³⁺ in Sm₂O₃ (the bottom spectrum in Fig. 1).

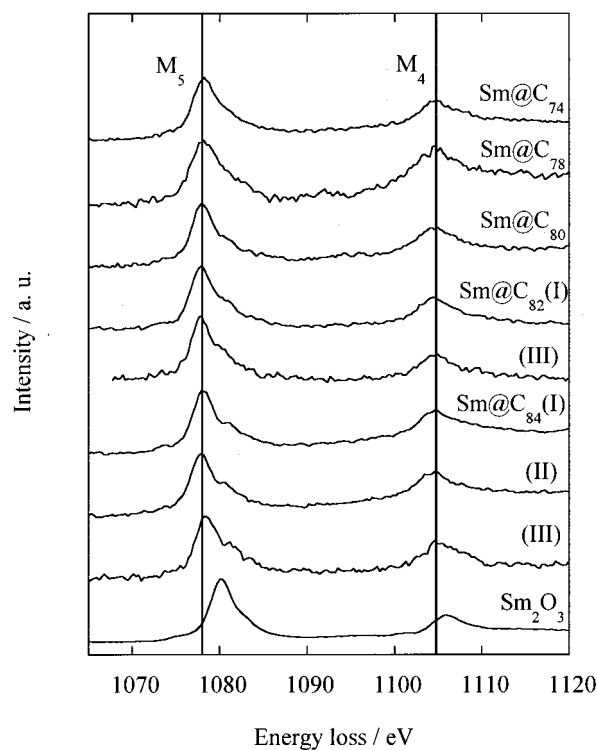
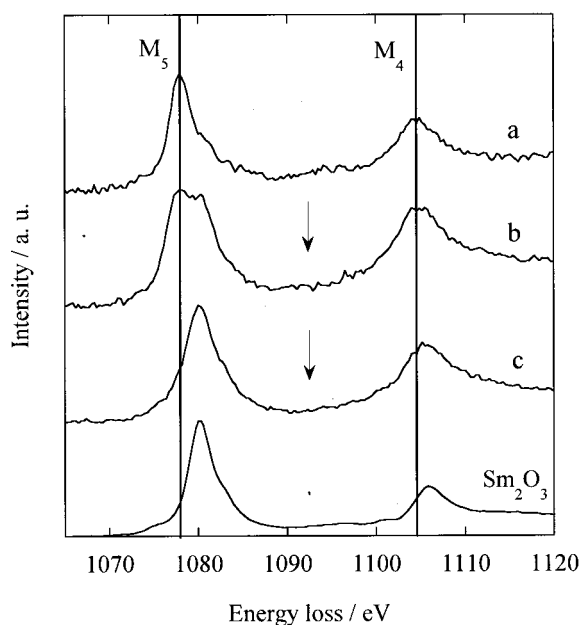


FIG. 1. EELS spectra of the Sm-containing metallofullerenes [Sm@C₇₄, Sm@C₇₈, Sm@C₈₀, Sm@C₈₂(I, III), Sm@C₈₄(I, II, III)] and trivalent Sm³⁺ in Sm₂O₃.

The shift value of the M_5 edge is 2.1~2.4 eV, which is almost identical to that observed for the XAS spectra of Sm²⁺ and Sm³⁺.^{17,18} The obtained EELS spectra have a broad side band in M_5 edge (~ 1081 eV). The fine structure of these patterns is governed by the density of $4f_{7/2}$ unoccupied states that are accessible to the $3d_{5/2}$ electron.¹⁸ Similar M_5 fine structure is also observed in the XAS spectrum published for a divalent Sm²⁺ in Sm_{0.3}Y_{0.7}S.¹⁷ Another possible origin of this peak is a small amount of the Sm³⁺ ion which forms as a result of the irradiation damage. Eventually, as discussed later, the Sm³⁺ signal will appear in a similar energy region during irradiation. The shape of this peak, however, is not clear because of the low experimental resolution. The obtained peak position of the side band (~ 1081 eV) is slightly higher than that of the major M_5 peak of Sm³⁺ (~ 1080 eV). Furthermore, the side peak can be also observed in an extremely weak irradiation condition, in which the Sm³⁺ signal does not appear even after the ~ 10 min. irradiation. We therefore conclude that the observed side band is the fine structure of the M_5 edge of divalent Sm²⁺. The present results indicate that the Sm atom takes a divalent state in Sm@C_{2n} [$2n = 74, 78, 80, 82$ (I, III), 84 (I, II, III)]. We will discuss the cage effect on the electronic state of metallofullerenes by using a simple thermochemical cycle model.

In the present experiment, the shape of the EELS spectra was changed with a lapse of the irradiation times of the electron beam. This trend can be observed in all the Sm metallofullerenes studied here. For example, Fig. 2 shows the time evolution of the spectrum of Sm@C₈₀. After the first mea-

FIG. 2. The time evolution of the EELS spectrum of Sm@C₈₀.

surement with the accumulation time of 1~2 min [Fig. 2(a)], intense peaks adjacent to the main peaks appeared [Fig. 2(b)]. In particular, the M_5 edge at ~1080 eV can be clearly seen in Fig. 2(b). The peak positions can be ascribed to those of Sm^{3+} .^{17,18} During the irradiation, the intensity of the divalent Sm^{2+} peaks decreased and finally disappeared [Fig. 2(c)]. This is indicative of the destruction of the fullerene cages by the irradiation of the electron beam. Obviously the Sm atom prefers to take +3 state outside the fullerene cage. In fact, the oxidation state of Sm atom is found to be +3 in samarium carbide (SmC_2).¹⁹ In this study, it is crucial to reduce the acquisition time for the valence state measurements to prevent irradiation damage which may mislead to a wrong conclusion for the valency.

B. A thermochemical cycle model

The present and previous⁶ results revealed that the Sm atom prefers to take +2 oxidation state in the fullerene cages [$\text{Sm}^{2+}@\text{C}_{2n}^{2-}$; $2n=74, 78, 80, 82(\text{I, II, III}), 84(\text{I, II, III})$]. On the other hand, group 3 and most of the lanthanide metallofullerenes generally take +3 states in the fullerenes.^{1-3,7} The preferential valency is, of course, reflected in a larger stability of the molecule. Here, we try to explain this cage size effect on the valency of Sm ion within a framework of the relative stability of the two electronic states ($\text{Sm}^{2+}@\text{C}_{2n}^{2-}$ and $\text{Sm}^{3+}@\text{C}_{2n}^{3-}$) by using a simple thermochemical cycle model [Fig. 3 (a)].

This thermochemical cycle model is similar to a model previously proposed by Wang *et al.*²⁰ In the first step of the thermochemical cycle [Fig. 3(a)], the Sm metal atom emits electrons and becomes Sm^{m+} state, where m is the valence of the Sm ion. This step requires activation energies corresponding to the sum of the ionization potentials of the Sm atom [$I_p^{\text{sum}}=I_p(\text{Sm}^+)+I_p(\text{Sm}^{2+})+\dots+I_p(\text{Sm}^{m+})$]. In the next step of the cycle, the electron, when transferred to

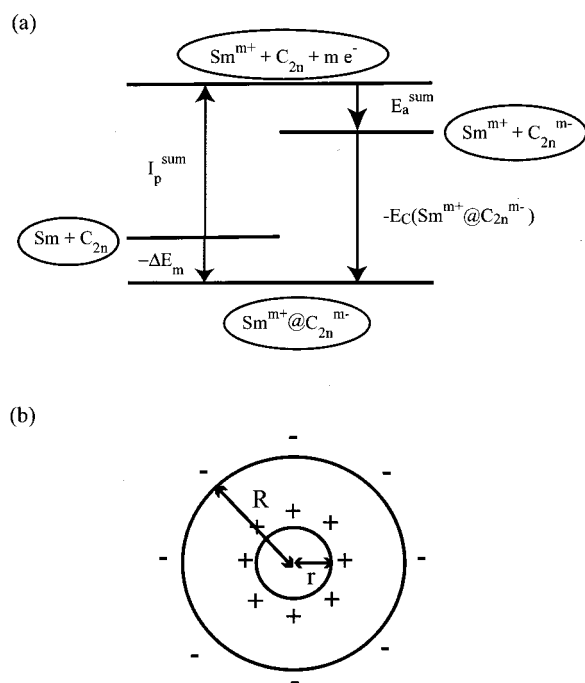


FIG. 3. Schematic illustrations of (a) a simple thermochemical cycle model and (b) a spherical shell model.

the fullerene cage, releases the energy given by the sum of the corresponding electron affinity [$E_a^{\text{sum}}=E_a(\text{C}_{2n}^-)+E_a(\text{C}_{2n}^{2-})+\dots+E_a(\text{C}_{2n}^{m-})$]. In the final step, the metallofullerene is further stabilized by a Coulomb attraction between the positive atom and the negative fullerene cage [$E_C(\text{Sm}^{m+}@\text{C}_{2n}^{m-})$]. Hence the stabilization energies, ΔE_m , during the formation of $\text{Sm}^{2+}@\text{C}_{2n}^{2-}$ (ΔE_2) and $\text{Sm}^{3+}@\text{C}_{2n}^{3-}$ (ΔE_3) are expressed as

$$\Delta E_2 = I_p(\text{Sm}^+) + I_p(\text{Sm}^{2+}) - E_a(\text{C}_{2n}^-) - E_a(\text{C}_{2n}^{2-}) + E_C(\text{Sm}^{2+}@\text{C}_{2n}^{2-}), \quad (1)$$

$$\Delta E_3 = I_p(\text{Sm}^+) + I_p(\text{Sm}^{2+}) + I_p(\text{Sm}^{3+}) - E_a(\text{C}_{2n}^-) - E_a(\text{C}_{2n}^{2-}) - E_a(\text{C}_{2n}^{3-}) + E_C(\text{Sm}^{3+}@\text{C}_{2n}^{3-}). \quad (2)$$

The relative stability between $\text{Sm}^{2+}@\text{C}_{2n}^{2-}$ and $\text{Sm}^{3+}@\text{C}_{2n}^{3-}$ ($\Delta E_{2 \rightarrow 3}$) is thus given by

$$\Delta E_{2 \rightarrow 3} = I_p(\text{Sm}^{3+}) - E_a(\text{C}_{2n}^{3-}) + \Delta E_C, \quad (3)$$

where $\Delta E_C = E_C(\text{Sm}^{3+}@\text{C}_{2n}^{3-}) - E_C(\text{Sm}^{2+}@\text{C}_{2n}^{2-})$.

Precise experimental data exist for $I_p(\text{Sm}^{3+})$ (=23.4 eV),²¹ whereas no reliable experimental values exist for $E_a(\text{C}_{2n}^{3-})$ of the large fullerenes. Hence we estimated this quantity from the energy level of the lowest unoccupied molecular orbital (LUMO) of C_{2n}^{2-} (Koopmans' theorem) by a semiempirical calculation. The geometrical structures of C_{2n}^{2-} were optimized at the PM3 level. The symmetries of the fullerene cages in $\text{Sm}@\text{C}_{74}$ and one of $\text{Sm}@\text{C}_{82}$ can be estimated to be D_{3h} and C_2 , respectively.⁶ Such structural information on $\text{Sm}@\text{C}_{78}$, $\text{Sm}@\text{C}_{80}$, and $\text{Sm}@\text{C}_{84}$ has been so far limited. Hence, in this calculation, we assumed that the symmetries of $\text{Sm}@\text{C}_{78}$, $\text{Sm}@\text{C}_{80}$, and $\text{Sm}@\text{C}_{84}$ cages are

TABLE I. The calculated third electron affinities [$E_a(C_{2n}^{3-})$], the estimated radii (R), the Coulomb interactions (ΔE_C) of various fullerene cages (C_{2n}), and the sum of the third electron affinity and the Coulomb interaction ($E_s = -E_a(C_{2n}^{3-}) + \Delta E_C$).

$2n$	$E_a(C_{2n}^{3-})/\text{eV}$	$R/\text{\AA}$	$\Delta E_C/\text{eV}$	E_s/eV
74	-2.5 (D_{3h}^a)	3.97	-18.1	-15.6
78	-2.4 (C_{2v}^a)	4.08	-17.7	-15.3
80	-2.2 (D_2^a)	4.14	-17.4	-15.2
82	-1.9 (C_2^a)	4.19	-17.2	-15.3
84	-1.7 (D_2^a)	4.25	-16.9	-15.2

^aThe symmetry of the calculated isomers.

the same as those of the most abundant isolated hollow fullerenes C_{2v} - C_{78} , D_2 - C_{80} , and D_2 - C_{84} , respectively.²²⁻²⁵ This assumption can be a good approximation for a qualitative understanding even if the fullerene cages of metallofullerenes generally have different symmetries from those of the corresponding hollow fullerenes.^{12,13} All calculations were carried out with the restricted Hartree-Fock (RHF) method. The singlet spin state for each C_{2n}^{2-} was assumed. The obtained $E_a(C_{2n}^{3-})$ values are negative because of the Coulomb repulsion between the electron and the charged cage (Table I). In Fig. 4, the $-E_a(C_{2n}^{3-})$ values are presented as a function of the number of the carbon atoms in the fullerene cage. As a general trend, the $-E_a(C_{2n}^{3-})$ values increase as the size of the fullerene decreases. This implies that the larger fullerene is a better electron acceptor than the smaller one.

The main part of the stabilization energy comes from the Coulomb attraction. We estimated this quantity by using a simple spherical shell model [Fig. 3(b)]. In this model, the metal atom and the fullerene cage are expressed as spheres with radii of r and R , respectively. The Coulomb interaction is given by $E_C(\text{Sm}^{m+}@C_{2n}^{m-}) = -m^2e^2/4\pi\epsilon_0R$, where ϵ_0 is a dielectric constant. The energy difference between E_C of $\text{Sm}^{2+}@C_{2n}^{2-}$ and $\text{Sm}^{3+}@C_{2n}^{3-}$ can, therefore, be expressed as $\Delta E_C = -5e^2/4\pi\epsilon_0R$. The radii of the fullerene cages (R) were estimated from the surface area of the fullerene. For example, C_{74} has 27 hexagons and 12 penta-

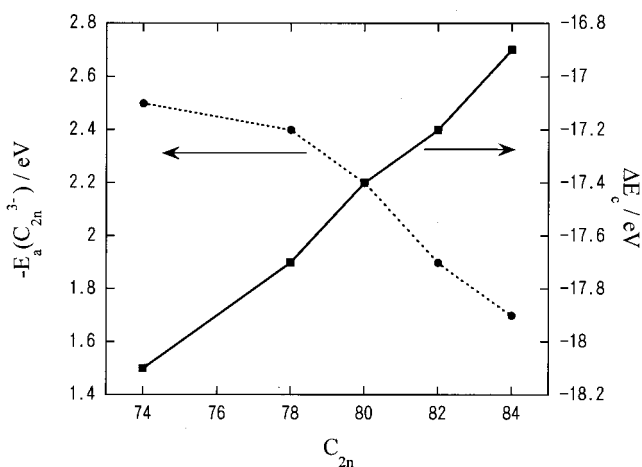


FIG. 4. The cage size effects on the estimated third electron affinities [$E_a(C_{2n}^{3-})$, solid circles] and the Coulomb interactions (ΔE_C , solid squares).

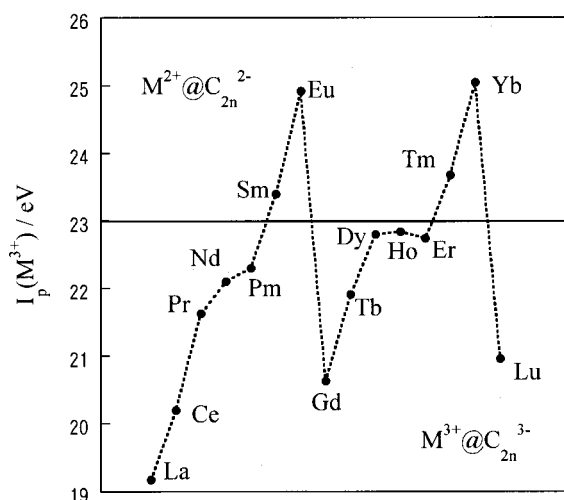


FIG. 5. The third ionization potentials [$I_p(M^{3+})$] of the lanthanide elements.

gons while C_{60} has 20 hexagons and 12 pentagons. Hence the relative ratio of the surface areas for C_{74} and C_{60} will be ~ 1.118 . Using this ratio and the experimental radius of C_{60} ($=3.55 \text{ \AA}$),²⁶ the radius (R) of C_{74} was estimated to be $\sim 3.97 \text{ \AA}$. The calculated radii of the other fullerenes by the method are listed in Table I. By using these values, ΔE_C was obtained for various sizes of fullerene cages from C_{74} to C_{84} (Table I). These calculations indicate that the ΔE_C value increases during the $+2 \rightarrow +3$ charge transfer process as the radius of the fullerene cage increases (Fig. 4).

C. The cage size effect on the oxidation state of the encapsulated Sm atom

The cage size effect on the relative stability between the two electronic states ($\text{Sm}^{2+}@C_{2n}^{2-}$ and $\text{Sm}^{3+}@C_{2n}^{3-}$) should appear in the third electron affinity of the cage [$E_a(C_{2n}^{3-})$] and the Coulomb interaction (ΔE_C). Table I also shows the sum of these energies ($E_s = -E_a(C_{2n}^{3-}) + \Delta E_C$) for each fullerene cage. As stated in Sec. III B, the stabilization energy from the Coulomb attraction (ΔE_C) becomes larger as the cage size decrease, whereas $-E_a(C_{2n}^{3-})$ exhibits an opposite trend (Fig. 4). Consequently, E_s will not become a sensitive function of the fullerene cage size.

It has been revealed that there is a correlation between $I_p(M^{3+})$ of the encapsulated metal and its oxidation state in a fullerene cage (Fig. 5).²⁷ The solid line around $\sim 23 \text{ eV}$ denotes a threshold. The atoms above this threshold prefer to take $+2$ oxidation states in the fullerene cages (group B) because a relatively high energy is needed to have $+3$ states, whereas the atoms below the threshold take $+3$ states inside the fullerenes (group A). The energetic difference between $I_p(M^{3+})$ of these groups is 0.58 eV [$=I_p(\text{Sm}^{3+}) - I_p(\text{Ho}^{3+})$], which exceeds the difference between the largest and the smallest E_s estimated above ($\sim 0.4 \text{ eV}$). This result implies that the oxidation states of the Sm ions do not change in the fullerene cages from C_{74} to C_{84} .

Recently, similar EELS measurements on a series of Sc dimetallofullerenes ($\text{Sc}_2@C_{2n}$, $2n=80\sim 90$) has also been carried out by the present group.²⁸ The observed peak position of the Sc *L*-edge is found to be almost identical for these molecules. Although the valency of the Sc atom in $\text{Sc}_2@C_{84}$ is still controversial,²⁹ these results indicate that the Sc atoms are trapped within the fullerenes with the same oxidation state. On these bases, we can conclude that the fullerene cage size effect on the electronic states of the encapsulated metal atoms is generally rather small.

The above simple model can explain the present experimental observation that the oxidation state of the Sm atom is insensitive to the fullerene cage. We should note, however, that this model provides us a qualitative understanding of the experimental results. For example, we cannot explain that group A atoms take +3 state in fullerenes by this model, i.e., $\Delta E_{2\rightarrow 3}$ of these metallofullerenes have positive values. This discrepancy may be due to the energy uncertainties for the individual steps described earlier. It is well-known that Koopmans' theorem provides a smaller E_a than the true value because in a real molecule the redistribution of electrons is occurring so as to relax the molecular structure. Hence the values of $E_a(C_{2n}^{3-})$ calculated here may be underestimated. Moreover, in a realistic description, the encapsulated metal atom does not locate at the center of the cage. Theoretical calculations^{30,31} showed that there is 2~3 eV of the energy gain from the off-center location in $\text{Sc}@C_{82}$ and $\text{La}@C_{82}$. A more detailed theoretical study is required to quantitatively describe the electron transfer process in metallofullerenes.

IV. CONCLUSION

We report a first systematic study of the varenity of the encapsulated metal in various fullerene cages by electron energy-loss spectroscopy (EELS). The resemblance of the EELS spectra of $\text{Sm}@C_{2n}$ [$2n=74, 78, 80, 82$ (I, III), 84 (I, II, III)] to those of a divalent Sm^{2+} in Sm alloys suggests that the Sm atoms take +2 valence states irrespective of the fullerene cages. This observation can be reproduced by our simple model with a thermochemical cycle. According to the model, the electron affinity increases as the fullerene size increases, whereas the gain in Coulomb interaction shows an opposite trend. This provides significant reduction of the cage size effect on the intramolecular electron transfer process of the metallofullerenes.

We also found that the Sm metallofullerenes can be converted to Sm carbide materials having Sm^{3+} states under a prolonged electron beam irradiation.

ACKNOWLEDGMENTS

The present work has been supported by Grants-in-Aid for Scientific Research (B)(2) (No. 12554026) by the Minis-

try of Education, Science, Sports and Culture of Japan and the Future Program on New Carbon Nano-Materials of the Japan Society for the Promotion of Science.

- ¹H. Shinohara, Rep. Prog. Phys. **63**, 843 (2000).
- ²S. Hino, H. Takahashi, K. Iwasaki, K. Matsumoto, T. Miyazaki, S. Hasegawa, K. Kikuchi, and Y. Achiba, Phys. Rev. Lett. **71**, 4261 (1993).
- ³S. Hino, K. Umishita, K. Iwasaki, T. Miyazaki, T. Miyake, K. Kikuchi, and Y. Achiba, Chem. Phys. Lett. **281**, 115 (1997).
- ⁴T. Pichler, M. S. Golden, M. Knupfer, J. Fink, U. Kirbach, P. Kuran, and L. Dunsch, Phys. Rev. Lett. **79**, 3026 (1997).
- ⁵K. Umishita, K. Iwasaki, S. Hino, M. Aoki, K. Kobayashi, S. Nagase, T. J. S. Dennis, T. Nakane, and H. Shinohara, Proceedings of the 16th Fullerene General Symposium 83, Okazaki, 1999 (unpublished).
- ⁶T. Okazaki, Y. Lian, Z. Gu, K. Suenaga, and H. Shinohara, Chem. Phys. Lett. **320**, 435 (2000).
- ⁷K. Kikuchi, K. Sueki, K. Akiyama, T. Kodama, H. Nakahara, I. Ikemoto, and T. Akasaka, in *Fullerenes, Recent Advances in the Chemistry and Physics of Fullerenes and Related Materials*, edited by K. M. Kadish and R. S. Ruoff (The Electrochemical Society, Pennington, NJ, 1997), Vol. 4, p. 408.
- ⁸H. Shinohara, in *Fullerenes, Recent Advances in the Chemistry and Physics of Fullerenes and Related Materials*, edited by K. M. Kadish and R. S. Ruoff (The Electrochemical Society, Pennington, NJ, 1997), Vol. 4, p. 467.
- ⁹T. J. S. Dennis and H. Shinohara, Chem. Phys. Lett. **278**, 107 (1997).
- ¹⁰T. J. S. Dennis and H. Shinohara, Appl. Phys. A: Mater. Sci. Process. **66**, 243 (1998).
- ¹¹T. Kato, S. Bandow, M. Inakuma, and H. Shinohara, J. Phys. Chem. **99**, 856 (1995).
- ¹²M. Takata, E. Nishibori, B. Umeda, M. Sakata, E. Yamamoto, and H. Shinohara, Phys. Rev. Lett. **78**, 3330 (1997).
- ¹³M. Takata, E. Nishibori, B. Umeda, M. Sakata, M. Inakuma, E. Yamamoto, and H. Shinohara, Phys. Rev. Lett. **83**, 2214 (1999).
- ¹⁴Y. Lian, Z. Shi, X. Zhou, X. He, and Z. Gu, Chem. Mater. (submitted).
- ¹⁵K. Suenaga, S. Iijima, H. Kato, and H. Shinohara, Phys. Rev. B **62**, 1627 (2000).
- ¹⁶GAUSSIAN 98W, M. J. Frisch, G. W. Trucks, H. B. Schlegel *et al.*, Gaussian Inc., Pittsburgh, PA, 1998.
- ¹⁷G. Kaindl, G. Kalkowski, W. D. Brewer, B. Perscheid, and F. Holtzberg, J. Appl. Phys. **55**, 1910 (1984).
- ¹⁸B. T. Thole, G. van der Laan, J. C. Fuggle, G. A. Sawatzky, R. C. Karnatak, and J.-M. Esteve, Phys. Rev. B **32**, 5107 (1985).
- ¹⁹T. Sakai, G. Adachi, T. Yoshida, and J. Shiokawa, J. Chem. Phys. **75**, 3027 (1981).
- ²⁰Y. Wang, D. Tománek, and R. S. Ruoff, Chem. Phys. Lett. **208**, 79 (1993).
- ²¹*CRC Handbook of Chemistry and Physics*, 80th ed. (CRC Press, Boca Raton, 1999).
- ²²F. Diederich, R. L. Whetten, C. Thilgen, R. Ettl, I. Chao, and M. M. Alvarez, Science **254**, 1768 (1991).
- ²³K. Kikuchi, N. Nakahara, T. Wakabayashi, S. Suzuki, H. Shiromaru, Y. Miyake, K. Saito, I. Ikemoto, M. Kainosho, and Y. Achiba, Nature (London) **357**, 142 (1992).
- ²⁴C.-R. Wang, T. Sugai, T. Kai, T. Tomiyama, and H. Shinohara, Chem. Commun. (Cambridge) 557 (2000).
- ²⁵T. J. S. Dennis, T. Kai, K. Asato, T. Tomiyama, H. Shinohara, T. Yoshida, Y. Kobayashi, H. Ishiwatari, Y. Miyake, K. Kikuchi, and Y. Achiba, J. Phys. Chem. A **103**, 8747 (1999).
- ²⁶K. Hedberg, L. Hedberg, D. S. Bethune, C. A. Brown, H. C. Dorn, R. D. Johnson, and M. de Vries, Science **254**, 410 (1991).
- ²⁷H. Huang and S. Yang, J. Phys. Chem. B **102**, 10196 (1998).
- ²⁸T. Okazaki, C.-R. Wang, K. Suenaga, and H. Shinohara (unpublished).
- ²⁹T. Pichler, Z. Hu, C. Grazioli *et al.*, Phys. Rev. B (in press).
- ³⁰S. Nagase and K. Kobayashi, Chem. Phys. Lett. **214**, 57 (1993).
- ³¹S. Nagase and K. Kobayashi, Chem. Phys. Lett. **228**, 106 (1994).